

Assessing chlorophyll-a retrieval of Sentinel-3 OLCI, VIIRS, MODIS and OC-CCI in Monterey Bay (California, USA)

Elliot Styles^{1*}, Lael Wakamatsu¹, Andrew M. Fischer¹

¹ Institute for Marine and Antarctic Studies – University of Tasmania (20 Castray Esplanade, Battery Point TAS 7004, Australia)

*Corresponding author: estyles@utas.edu.au

ABSTRACT

Advances in high-resolution satellite sensors and merged multi-sensor ocean colour products have improved the detection of submesoscale features and enhanced the continuity of ocean surface measurements. This has enabled more detailed observations of chlorophyll-a (chl-a) growth rates, biomass and biogeochemical fluxes. Chl-a, a photosynthetic pigment in marine autotrophs, is used as a proxy for phytoplankton biomass and primary productivity. The accurate estimation of surface chl-a via remote sensing is key to improving coastal ocean process modelling. We compared chl-a products from sensors of multiple spatial resolutions, including Sentinel-3 Ocean and Land Colour Imager (OLCI), the Moderate Resolution Imaging Spectroradiometer (Aqua) (MODIS Aqua), the Visible Infrared Imaging Radiometer Suite (VIIRS) on Suomi NPP and the Ocean Colour Climate Change Initiative (OC-CCI) V6 product to two *in situ* datasets (M1 and C1) in Monterey Bay, California, USA. Sentinel-3 consistently performed well under the Inverse Modelling Technique - Neural Network chl-a algorithm, performing slightly better at station M1 ($R^2_{M1} = 0.85$, $R^2_{C1} = 0.80$). The Ocean Colour for MERIS algorithm performed better at offshore station M1 ($R^2_{M1} = 0.87$) and yielded no matchups at C1. MODIS Aqua and VIIRS performed poorly ($R^2_{M1,MODIS} = 0.32$, $R^2_{M1,VIIRS} = 0.02$, $R^2_{C1,MODIS} = 0.08$, $R^2_{C1,VIIRS} = 0.25$), likely inhibited by calibration to global as opposed to regionally adapted datasets. OC-CCI, though blended for greater continuity, produced fewer matchups at a higher accuracy ($R^2_{M1,OC-CCI} = 0.66$, $R^2_{C1,OC-CCI} = 0.63$) than MODIS Aqua or VIIRS alone, but still less so than Sentinel-3 OLCI. All sensors either over- or under-estimated chl-a at all concentrations, apart from OC-CCI, likely due to the complex coastal optical properties of the area. Our results highlight the need for regional algorithm development and show the potential effectiveness of Sentinel-3 and OC-CCI products for future submesoscale process studies.

Keywords: Ocean colour, Remote sensing, Chlorophyll-a, Sentinel, MODIS Aqua, OC-CCI

INTRODUCTION

Remote sensing (RS) applications typically enable us to make Earth observations at regional and global scales, with open-source data offering free access worldwide. The development of higher resolution satellite sensors and blended

products has provided the ability to monitor finer submesoscale processes in coastal waters using chlorophyll-a (chl-a). Chl-a is a pigment in autotrophic organisms that provides a proxy for biomass, which can be used to infer ecosystem health by estimating primary productivity (Azmi et al., 2015; Friedland et al., 2012; Torbick et al., 2008). Autotrophs are the primary food source for higher trophic levels and a major source of sequestration of atmospheric CO₂. They accumulate carbon via photosynthesis and store it in sediments (Joint and Groom, 2000;

Submitted: 10-Dec-2023

Approved: 15-Apr-2025

Editor: Rubens Lopes



© 2025 The authors. This is an open access article distributed under the terms of the Creative Commons license.

Polimene et al., 2017). This process locks away about 30% of anthropogenic CO₂ emissions, serving as a critical buffer against climate change in general. Therefore, improved (including higher-resolution and finer-scale) measurements of phytoplankton activity are vital to understand and model submesoscale processes and inform management and scientific efforts (Basu and Mackey, 2018; Divya et al., 2018).

In general, challenges arise using RS for chl-a estimation, such as atmospheric correction (Werdell et al., 2010), cloud cover (Markelin et al., 2016), coarse spatial and temporal resolutions (Giardino et al., 2014) and complex coastal optical properties (i.e., turbidity, river input and land-sea ambiguity), affecting satellite image quality, retrieval algorithms and thus data reliability (Chen et al., 2013). Waters characterized by multiple factors influencing their optical properties (i.e., non-algal particles (NAPs) and coloured dissolved organic matter (CDOM)), such as coastal and inland areas, are referred to as Case 2 waters. In contrast, open ocean regions, in which surface optical properties are primarily influenced by photosynthetic pigments (i.e., chl-a) are known as Case 1 waters, as per the optical classification described by Morel and Prieur (1977) (Chen et al., 2013; Darecki et al., 2003; Sorrell et al., 2009). Depending on the sensor, raw optical images are often processed by algorithms, such as Ocean Chlorophyll 2 (OC2), a two-band empirical algorithm for chl-a concentration retrieval from RS reflectance (Tilstone et al., 2021). Product variability occurs between sensors, with some, such as Sentinel-3 (S3), focusing on higher spatial resolutions (i.e., 300m), whereas others, such as the moderate resolution imaging spectroradiometer (Aqua) (MODIS Aqua), focus on high temporal coverage (i.e., 1 day; Table 1). Conventionally, achieving high spatial and temporal resolution with consistent coverage has proven challenging due to inherent trade-offs, associated with specific scientific objectives and engineering compromises. To produce consistent and complete error-characterized time-series data for climate research and modelling, blended products (OC-CCI) have been developed. These products were designed to provide improved temporal and spatial coverage by blending data from satellite missions and reduce gaps due to

cloud cover and to minimize sensor degradation or limited swath width. Blended products also reduce bias and enhance the reliability of chlorophyll concentration estimates (Valente et al., 2022).

S3 Ocean and Land Colour Instrument (OLCI) imagery has been used to derive accurate estimates of chl-a ($R^2 = 0.83$, RMSE = 9.8 mg/m³) using *in situ* data in a Baltic Lake study (Soomets et al., 2020). Additionally, S3 has been suggested for use with higher concentrations (>20 mg/m³); both have been found to outperform MODIS Aqua and VIIRS when using commonly applied algorithms such as OC2/OC3 (Cazzaniga et al., 2019; Pirasteh et al., 2020; Tilstone et al., 2021). S3 has proven most accurate in turbid areas, such as the Belgian and the Mediterranean coastlines, when processed using specialty bio-optical algorithms, alongside specific atmospheric corrections via RS data processing applications such as ACOLITE (Sòria-Perpinyà et al., 2021; Vanhellemont and Ruddick, 2021). Both MODIS Aqua and the visible infrared imaging radiometer suite (VIIRS) on Suomi NPP have shown promising results in Case 2 waters, such as the Arabian Gulf (MODIS Aqua $R^2 = 0.79$) and Chinese waterways (VIIRS $R^2 = 0.76$), when combined with area-specific algorithms (Al-Naimi et al., 2017; Jiang et al., 2020). These studies have provided a baseline for sensor accuracy. However, a localized comparison of the three has yet to be conducted in more turbid and productive Case 2 waters. For the open ocean, chl-a concentrations are typically derived utilizing reflectance and absorption in the blue and green portion of the electromagnetic spectrum. However, coastal and inland settings often show an overlapping of absorption characteristics between chl-a with NAPs and CDOM, making it difficult for bio-optical algorithms to derive accurate estimates (Herman, 1999; Lin et al., 2014; Nima et al., 2016). Adding to this, turbidity, chl-a, NAP and CDOM properties are highly variable. Thus, it is necessary to validate chl-a algorithms for RS sensors in several regions to determine accuracy and help guide the future development of regionally unique algorithms (Al-Naimi et al., 2017; Darecki et al., 2003; Theenathayalan et al., 2022).

In this study, we analysed and compared the chl-a products from four ocean colour sensors (MODIS Aqua, VIIRS, S3 OLCI

and the OC-CCI V6 merged multi-sensor ocean colour product) (Sathyendranath et al., 2023) (Table 1) regarding *in situ* data measured via laboratory optical fluorometry collected from fixed long-term sampling locations in coastal Monterey Bay, California, USA (Figure 1). This range of sensors represents distinctly varying spatial and temporal resolutions, which provides a comparison for assessing the use of a specific sensor to observe coastal processes across multiple spatial scales. Additionally, all sensors have varying numbers of spectral bands, which affects the quality, reliability, and range of optical properties that can be derived from a sensor. S3 (OLCI) has 21 spectral bands, MODIS Aqua has 36 and VIIRS has 22. OC-CCI V6 is a blended product combining the common bands of the various sensors; yet this quantitative measure is not purely indicative of the accuracy of derived products (Barnes and Salomonson, 1992; Jackson, 2020; Sathyendranath et al., 2012; Schueler et al., 2002).

Another source of variation occurs from the product algorithms. MODIS Aqua and VIIRS

products are commonly derived using the colour index algorithm (CIA), which is based on empirical measurements of *in situ* chl-a and RS reflectance within the green and blue spectra (Hu et al., 2012; Kahru et al., 2015; O'Reilly et al., 1998). Lastly, two commonly applied algorithms to S3 ocean imagery are ocean colour for the Medium Resolution Imaging Spectrometer (MERIS) (OC4Me) and inverse modelling with neural networks (NN). OC4Me is a polynomial semi-analytical algorithm based on a history of apparent optical properties that are measured *in situ* around global coastal waters (Bricaud et al., 1998; Morel and Maritorena, 2001; Morel et al., 2007). The NN approach is different to the other algorithms, using an inverse radiative transfer model neural network that trains the model rather than being based on empirical or analytical analyses (Brockmann et al., 2016; Schiller and Doerffer, 1999; Syariz et al., 2019, 2020). OC-CCI is a merged multi-sensor product, created to increase continuity of measurements (Sathyendranath et al., 2023).

Table 1. Satellite date ranges with temporal (hrs/days) and spatial (km² or m²) resolutions.

Sensor	Date Range	Temporal Resolution	Spatial Resolution	Algorithm
OC-CCI	September 1997 – Present	1 Day	1 km ²	V6
MODIS Aqua	May 2002 – Present	1 Day	1 km ²	CIA
VIIRS	October 2011 – Present	1 Day	750 m ²	CIA
Sentinel-3	May 2016 – Present	1-2 Days	300 m ²	OC4Me/NN

STUDY SITE

Approximately 40 km wide at the mouth and covering an area of around 100 km², Monterey Bay is the largest open bay in coastal California (Ryan et al., 2009). Monterey Bay lies in the central California Current System, a biologically productive region created by the coastal upwelling of cold nutrient-rich waters along the western coast of the US (Ryan et al., 2009; Manzer et al., 2019). Monterey Bay is of specific interest due to the near-shore deep-water canyon that begins at the mouth of the Elkhorn Slough, helping to facilitate upwelling and sustaining diverse marine communities (Goffredi et al., 2004; Mansergh and Zehr, 2014; Rosenfeld et al., 1994). This seasonal upwelling in Monterey

Bay begins at the start of spring, inciting large, productive phytoplankton blooms (Breaker, 2005; Reji et al., 2020). This boom in productivity leads to post-upwelling relaxation periods as the water column becomes thermally stratified before the onset of the poleward flowing Davidson Current in winter, bringing warmer water and reducing stratification, decreasing phytoplankton bloom regularity and scale (Chavez, 1996; Pennington and Chavez, 2000; Reji et al., 2020; Ryan et al., 2014; Thomson and Krassovski, 2010). As with all coastal regions, physical processes in Monterey Bay operate across a variety of temporal and spatial scales and concentrations of chl-a are largely driven by seasonal upwelling (Manzer et al., 2019).

The long-running marine research in the region, primarily coordinated by the Monterey Bay Aquarium Research Institute (MBARI), has seen the deployment of multiple permanent *in situ* long-term sampling stations from which oceanographic data are collected. In total, two locations of interest for this study are M1 and C1; approximately 5 and 20 km from the coast (Figure 1) (Mansergh and Zehr, 2014). These locations are visited monthly from which

water samples are taken for chl-a measurements. This high biological productivity, coupled with the long-term record of *in situ* chl-a, makes Monterey Bay an ideal location to conduct a sensor validation study, especially to test the accuracy of commonly employed sensors and algorithms in a coastal setting. While the station at M1 is exposed to the conditions of the offshore California Current, the station at C1 represents coastal Case 2 waters.

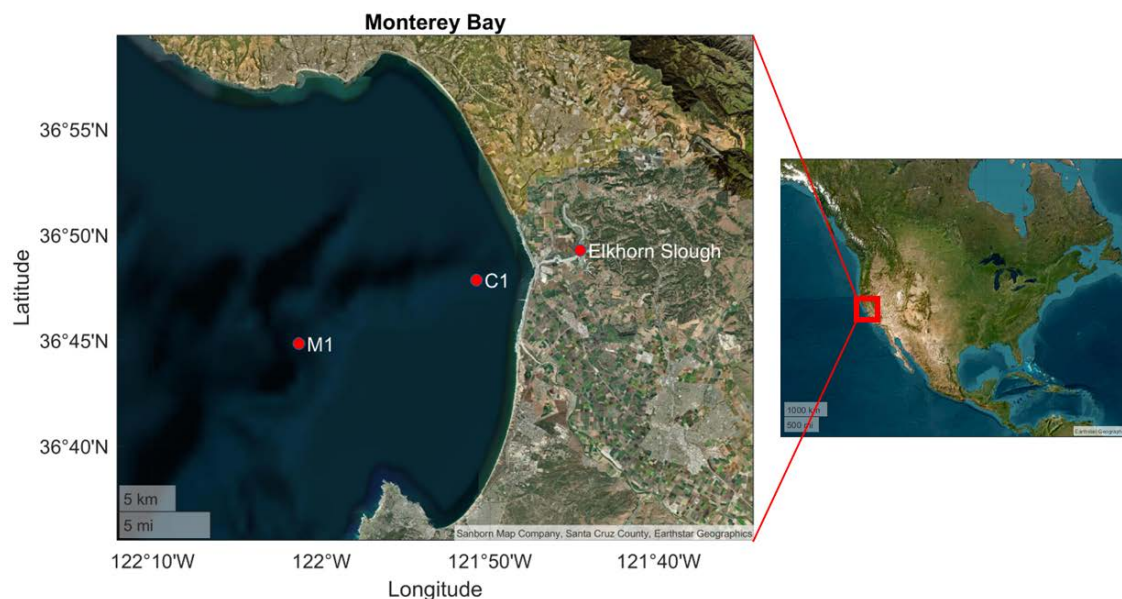


Figure 1. *In situ* sampling locations within Monterey Bay, California, USA. The Elkhorn Slough has been annotated for reference as the start of the deep-sea canyon above which the two locations of the M1 and C1 are situated.

AIMS

This investigation aimed to assess the accuracy of chl-a products from four sensors, coupled with their algorithms, against *in situ* data in the Case 2 waters of Monterey Bay. Its outcome will aid recommendations to guide future studies of coastal RS and the applications of global algorithms to regional areas. Furthermore, it will help to assess the accuracy of higher resolution and blended RS products that may explain finer and submesoscale oceanographic processes. This investigation aims to:

1. Find the most accurate sensor and algorithm for a) near-shore (i.e., C1) and b) coastal regions (i.e., M1).

2. Describe the variance in accuracy of chl-a retrieval as influenced by sensor characteristics or various algorithms.

METHODS

DATA COLLATION

In situ chl-a data were obtained from the Biological Oceanography Group at MBARI, who took seawater samples at the M1 and C1 stations. Chl-a concentrations were assayed using the modified fluorometric procedure of Holm-Hansen et al. (1965). Chl-a was extracted from glass microfiber filters (grade GF/F, pore size 0.7 μm) through which known volumes of seawater collected with a CTD rosette had been passed

using 10 ml of 95% acetone, stored in a freezer between 24 to 30 hours once the sampling trip returned to shore. Fluorescence of the extracted chl-a was measured using a Turner Designs Model 10-005 R fluorometer calibrated using known concentrations of commercial chl-a. Chl-a for each sample was then calculated from the standard curve relating fluorescence and chl-a (Holm-Hansen et al., 1965; Parsons et al., 1984; Pennington and Chavez, 2000). Optical satellite data were sourced to match *in situ* data from 1 January, 2013 to 1 July, 2021. MODIS Aqua and VIIRS have daily one-km resolution L2 data that were sourced from the 'from the National Aeronautics and Space Administration (NASA) repository WorldView with the CIA algorithm applied (Hu et al., 2012). Daily, 300-m resolution S3 imagery was downloaded from the European Organisation for the Exploitation of Meteorological Satellites, including OC4Me and NN chl-a products. OC-CCI data were downloaded from its portal (<https://www.oceancolour.org/portal/>).

DATA PROCESSING

For the OC-CCI, MODIS Aqua, VIIRS and S3 data sets, the pixels within a three by three window (i.e., pixel size is equal to the spatial resolution of the sensors; see Table 1) surrounding the *in situ* stations were found and extracted, and the mean chl-a value was calculated and used for analysis. Once the chl-a values were spatially extracted, the mean chl-a value of each sensor was matched to the corresponding *in situ* point based on date. Matchups were allocated between points that were captured within \pm three hours of each other, ensuring that temporally reasonable matches could be made without sacrificing the sample size for each sensor. For MODIS and VIIRS processing, ATM_FAIL, LAND, HIGLINT, STRAYLIGHT, CLDICE, HISOLZEN and HISATZEN flags were applied (Table S1). The 869-nm channel was applied for cloud flagging over water. For S3 OLCI, the following set of common quality flags were used: AC_FAIL and INVALID, CLOUD, CLOUD_AMBIGUOUS, CLOUD_MARGIN, SNOW_ICE, COSMETIC, SATURATED, SUSPECT, HISOLZEN, HIGHGLINT, ADJAC and WHITECAPS (Table S2). OC-CCI V6 is a merged product that was adopted for generating

an ocean-colour time series for climate studies using data from the MERIS sensor of the European Space Agency, the sea-viewing wide-field-of-view sensor (SeaWiFS) and MODIS-Aqua sensors from the NASA (USA) and the VIIRS from the National Oceanic and Atmospheric Administration (USA). More information on the algorithm development and processing can be found in Sathyendranath (2023).

DATA ANALYSIS

The matchups were evaluated by fitting a linear regression to the data for each sensor and *in situ* combination, in which the R^2 , root mean squared error (RMSE), bias and residual prediction deviation (RPD) were used to appraise the fit of the remotely sensed values. RPD involves dividing the standard deviation of observed values by the RMSE of prediction. It is a non-dimensional statistic that can be used to evaluate model validity and can be more easily compared across different model validation studies. A greater RPD indicates a better predictive capacity of a model. The relative percent difference (RPD (%)) between satellite estimates and *in situ* values was also calculated. All analyses were applied to log-transformed data, owing to the natural distribution of chl-a on a logarithmic scale, and that this transformation downweights large values to more easily capture fine scale trends (Campbell, 1995).

RESULTS

Table 2 compares the sensors and algorithms used at two stations, M1 and C1. For station M1, the best performing algorithms were S3 OC4Me and NN, having the highest R^2 values ($R^2_{S3(OC4Me),M1} = 0.87$; $R^2_{S3(NN),M1} = 0.85$) and indicating a good model fit (Table 1). The merged OC-CCI V6 product shows reasonable performance ($R^2_{OC-CCI,M1} = 0.66$), with the VIIRS CIA algorithm performing poorly ($R^2_{MODIS(CIA),M1} = 0.02$). For station C1, S3(NN) and OC-CCI V6 obtained the best R^2 values ($R^2_{S3(NN),C1} = 0.80$; $R^2_{OC-CCI,C1} = 0.63$). MODIS Aqua (CIA) performed the worst at C1 ($R^2_{MODIS,C1} = 0.08$), giving the CIA algorithm almost no predictive power. VIIRS CIA also performed poorly at M1 and C1 ($R^2_{VIIRS(CIA),M1} = 0.02$; $R^2_{VIIRS(CIA),C1} = 0.25$). RMSE and bias

values indicate model performance and over- or under-prediction. Highest RMSE values or poor performance pointed to MODIS Aqua CIA at M1 (RMSE = 30.1) and MODIS and VIIRS CIA at C1 (RMSE = 5.9 and 5.2). The MODIS Aqua CIA algorithm at C1 had a bias of 3.4, showing a strong over-/under- prediction at M1 (RMSE = 5.2). S3 OC4Me at M1 had a bias of 3.4 and S3 NN had a bias of 5.5 at M1 and C1, indicating over-prediction. A highly positive RPD (%) for S3 OC4Me (M1, 99%) and S3 NN (M1, 121% and C1, 120%) indicated a large discrepancy between the *in situ* and satellite derived values. VIIRS and MODIS CIA (M1, 216% and C1, 165%) had the highest RPD (%). Overall, S3 OC4Me and S3 NN models had the best R² for M1 but suffered from high RPD (%) and bias. MODIS Aqua and

VIIRS CIA remain unreliable at M1 and C1, with low R² values. OC-CCI V6 is a stable performer across both stations. The RPD indicated that the best performance occurred with the OC-CCI V6 algorithm at stations M1 and C1 (RPD = 1.4 and 1.7). The poorest predictive performance at M1 occurred with VIIRS CIA (RPD = 0.51) and at C1 with the MODIS Aqua CIA (RPD = 0.22). In summary, the best model, S3 OC4Me, had the highest R² (0.87), despite its slightly high bias. The worst models are VIIRS CIA, an extremely poor performer at M1 and MODIS Aqua CIA, a poor performer at C1. OC-CCI V6 (R² = 0.63 - 0.66, RMSE = 1.5 - 1.8, RPD = 1.4 - 1.7) showed a good balance of accuracy and low bias. S3 models (OC4Me, NN) showed strong predictive power but require bias correction.

Table 2. Total correlations, R², RMSE, Bias, RPD (%) and RPD for each sensor and algorithm at the M1 and C1 stations. * denotes a statistically significant result ($p < 0.05$).

Station	Sensor	Algorithm	n	R ²	RMSE	Bias	RPD (%)	RPD	Comments
M1	OC-CCI	V6	17	0.66*	1.8	1.0	22	1.4	Moderate R ² , low RMSE, good RPD and reasonable bias. Performs well.
	MODIS Aqua	CIA	24	0.32*	30.1	5.2	94	1.0	Low R ² , very high RMSE and high bias. Poor predictive performance.
	VIIRS	CIA	12	0.02	6.6	1.8	216	0.51	Extremely low R ² and high error rates. Poor model fit.
	S3	OC4Me	9	0.87*	4.2	3.4	99	0.75	Best R ² but high RMSE and bias. Decent model but needs bias correction.
	S3	NN	11	0.85*	7.9	5.5	121	0.82	High R ² but high RMSE and bias. Good predictive power but systematic overestimation.
C1	OC-CCI	V6	17	0.63*	1.5	0.17	56	1.7	Good R ² , lowest RMSE and minimal bias. Best overall balance.
	MODIS Aqua	CIA	21	0.08	5.9	3.4	165	0.22	Very low R ² and high RMSE. Poor predictive performance.
	VIIRS	CIA	29	0.25	5.2	0.52	50	1.0	Low R ² but acceptable RPD. Moderate accuracy.
	S3	OC4Me	0	--	--	--	--	--	No data available.
	S3	NN	11	0.80*	7.9	5.5	120	0.82	High R ² , but high RMSE and bias. Similar to M1.

The regression plots in Figure 2 provide a key insight into the over- or underestimation of the sensors and algorithms. The variability in blue points across plots suggests that the algorithms/sensors have varying degrees of agreement with *in situ* data. If the regression line (solid orange)

deviates from the 1:1 red dashed line, it indicates systematic bias. The dotted lines surrounding the regression line estimates uncertainty; wider intervals suggest higher variability. OC-CCI V6 fits reasonably well the 1:1 line, with a slight overestimation of *in situ* chlorophyll at M1 and C1.

VIIRS and MODIS Aqua tend to underestimate it at higher concentrations and to overestimate it at lower values. MODIS Aqua and VIIRS seem to have higher variability in satellite-derived chl-a values against *in situ* data when compared

to other satellites. MODIS Aqua has more scattering, suggesting higher uncertainty. The S3 algorithms seem to consistently overestimate chl-a values. Note the change in the axes of these algorithms in Figure 2.

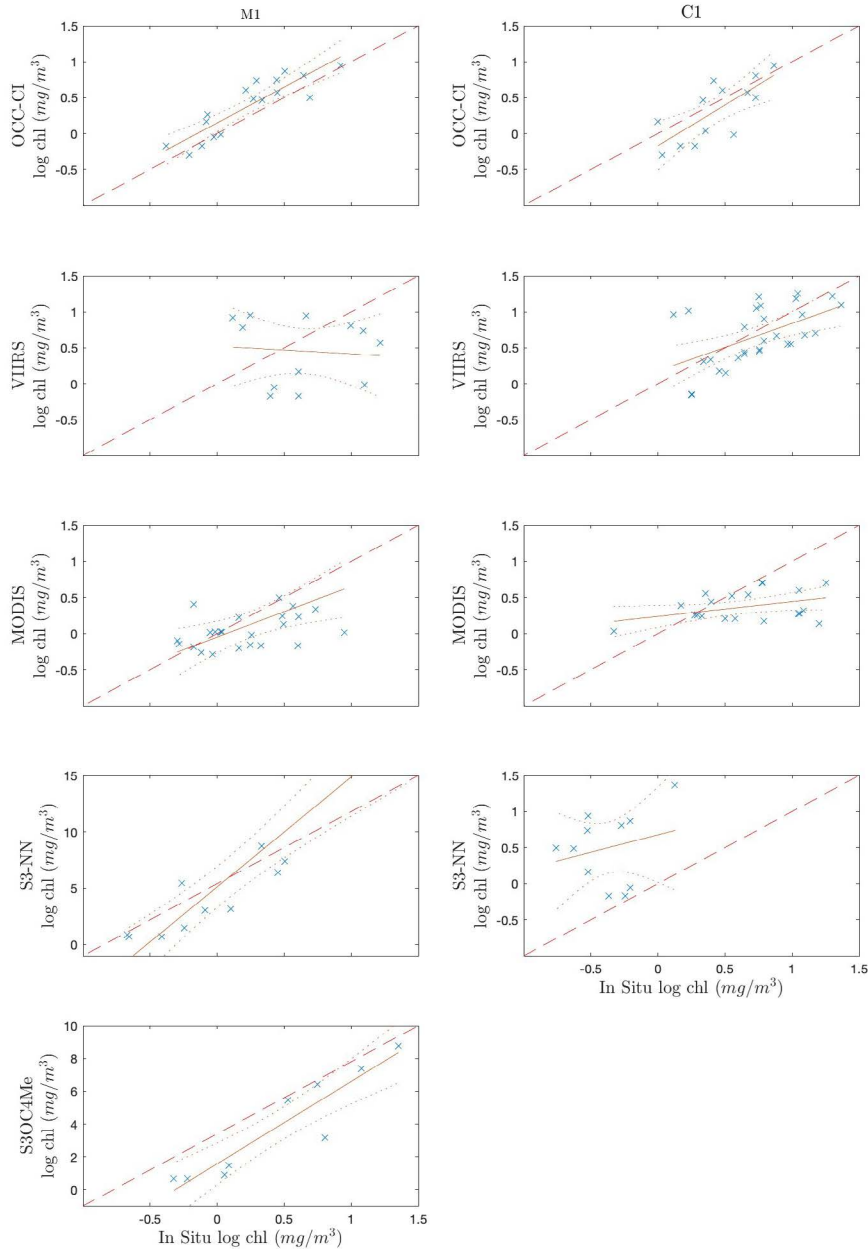


Figure 2. Scatter plot of the log chl-a for each combination of *in situ* sample location (x axis) and sensor (y axis) that was regressed, with 95% confidence intervals shown in orange dotted lines. The blue points represent matchups between satellite-derived and *in situ* measurements. The solid orange line is a regression fit indicating the general trend of the relationship. The dotted lines represent confidence intervals. The red dashed line represents the 1:1 relationship, which indicates perfect agreement between the satellite and *in situ* data. Note the change in scale for the y-axis for S3 NN and S3 OC4Me at station M1.

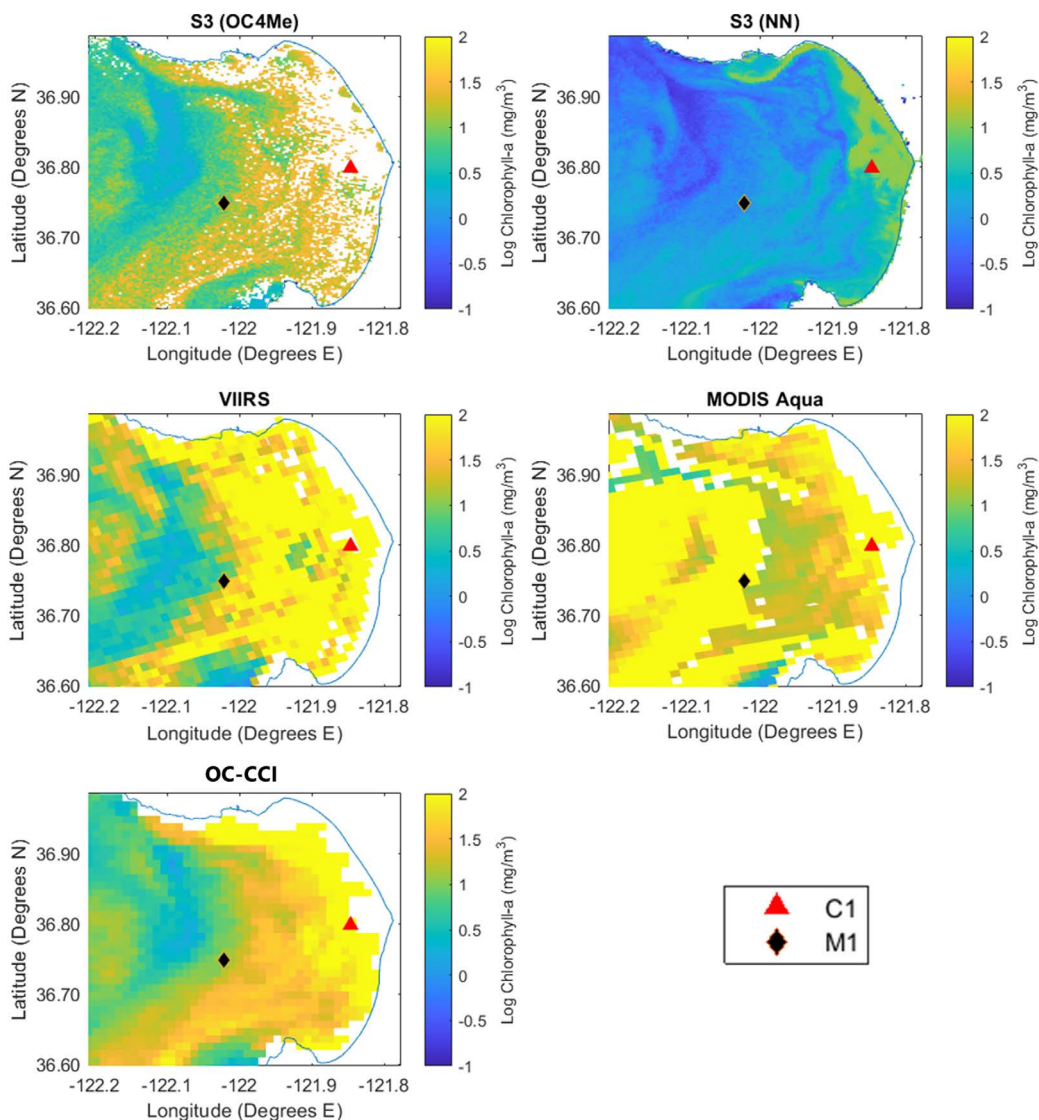


Figure 3. Log chl-a (mg/m³) product at Monterey Bay on 12 September, 2019 from S3 (OC4Me & NN), VIIRS, MODIS Aqua and OC-CCI. White pixels denote no chl-a measurement from cloud cover and coarse resolution near the coast.

Figure 3 provides spatial insight into chl-a estimation between sensors with a matchup of sensors on September 12th, 2019. The NN algorithm for S3 could derive chl-a values less than two km from the shoreline in Monterey Bay. Comparatively, S3 OC4Me seemed to encounter difficulty deriving values that were closer to the shoreline, and the image also showed patchiness. VIIRS and MODIS Aqua also showed patchy coastal estimations (up to ~2-3 km offshore). OC-CCI faced a similar difficulty to MODIS Aqua and VIIRS with nearshore

retrievals. This figure indicates that the NN on S3 was the most conservative (i.e., -1 to 1 on a log scale), followed by OC4Me and OC-CCI. VIIRS and MODIS Aqua derived very high values (i.e., 2 on a log scale) when compared to S3.

DISCUSSION

Sensor correlations with *in situ* measurements varied depending on the combination of sensors, algorithms and sampling locations. MODIS Aqua and VIIRS had the least accurate measurements,

particularly at C1, and S3 returned moderate results for both algorithms (OC4Me and NN). OC-CCI returned the best overall matchups for both sensors based on all validation metrics. A general marked decline in performance at C1 occurred when compared to M1, which can be attributed to the turbid nature of the coastal sampling location as algorithms based on the blue-green wavelengths can fail due to scattering and absorption by CDOM (Ansper and Alikas, 2018). Our results also vary according to other studies conducted on the same sensors in optically complex waters.

OC-CCI VERSION 6 (v6)

OC-CCI performed, on average, the best (Table 3) in this comparison study. At M1 and C1, OC-CCI showed a strong balance between accuracy, bias correction and RPD. Other validation studies using OC-CCI are limited. However, a recent application by Wakamatsu et al. (2022) in Tasmania, Australia, yielded similar results to this study. When comparing three chl-a datasets (VIIRS, MODIS Aqua and OC-CCI), OC-CCI performed the best for waters around the east coast of Tasmania. However, it was difficult to determine if OC-CCI chl-a was one of the strongest matches to *in situ* data overall since the matchups around Tasmania were weak and applied in very localized areas (Wakamatsu et al., 2022). The strength of OC-CCI, however, is that being a blended product, it helps to fill temporal and spatial gaps in locations in which other sensors are fixed (Table 1). Therefore, we suggest that OC-CCI V6 could be applied when imaging optically complex waters as our comparison indicates that it is a reliable baseline algorithm.

SENTINEL-2 AND SENTINEL-3

Sentinel-2 (S2) is included to provide further context to this study as the number of matchups ($n = 4$) that occurred are too few to include in the main results of this research (Table 3). The S2 performance for both algorithms (OC2 and OC3) showed reasonable correlations, in line with recent studies on chl-a retrieval in turbid lake settings in Vietnam ($R^2 = 0.68$), Lake Huron ($R^2 = 0.49$), Kaštela Bay in Croatia ($R^2 = 0.69$) and the central Italian Tyrrhenian coast ($R^2 = 0.55$), evincing the performance of S2, particularly at C1 (Chen et al., 2017; Ha et al., 2017; Ivanda et al., 2021; Orlandi et al., 2018). Shaik et al. (2021) achieved improved satellite retrieval ($R^2 = 0.88$) for the Kakinada and Yanam turbid coastal waters along the east coast of India using fluorescence line height and maximum chlorophyll index algorithms. These studies, among others, attribute the success of S2 to its fine spatial resolution (Ansper and Alikas, 2018). While our limited results agree with the findings of other studies, we are ultimately unable to draw meaningful conclusions due to the small sample size for both algorithms under S2 and its associated high bias and RPD. Additionally, the large underestimation of S2 likely offers an avenue for speculation regarding the accuracy of the sensor under the OC2 and OC3 algorithms in Case 2 waters. Increasing the number of data points for S2 would require inflating the *in situ* matchup window up to potentially ± 24 hours. While this would increase the sample size for all sensors, the accuracy of any derived chl-a would likely decline. This is an important trade-off to consider, especially in the context of a sensor comparison study in Case 2 waters.

Table 3. Sensor results from Sentinel-2 at M1 and C1 with the OC2 and OC3 algorithms. The lack of matchups meant that this sensor and the algorithms used were excluded from the main results section.

Station	Sensor	Algorithm	<i>N</i> Matchups	R2	RMSE	BIAS	RPD (%)
M1	S2	OC2	4	0.88	0.10	1.9	64
	S2	OC3	4	0.84	0.10	2.4	91
C1	S2	OC2	4	0.93	0.12	5.2	120
	S2	OC3	4	0.95	0.14	5.5	138

It is difficult to completely align our results for S3 (both OC4Me and NN) with the existing literature as the sensor performed differently at M1 and C1,

with OC4Me failing to retrieve any matchups at C1. A coastal study in the Mediterranean Sea found that OC4Me showed an overall moderate correlation

with *in situ* points ($R^2 = 0.55$), outperforming NN, which obtained poorer results (Moutzouris-Sidiris and Topouzelis, 2021). Our results agreed with this study, as OC4Me outperformed NN at M1, a site further offshore influenced by the oceanic waters of the California Current. Another study conducted in the Atlantic Meridional Transect, which includes coastal waters, found that S3 underestimated chl-a at low concentrations, in line with our results, except that all values were underestimated in our case (Tilstone et al., 2021). Similar to our results, Binh et al. (2022) found R^2 values of 0.58 for the OC4Me algorithm in Vietnamese coastal waters (Case 2), and Staehr et al. (2023) found an $R^2 = 0.56$ for Danish coastal seas. Despite these moderate R^2 values, it is clear from our results that these sensors with finer spatial resolutions can differentiate and identify finer submesoscale oceanographic processes in these waters. As such, we propose that potential users should consider the NN algorithm due to its high predictive power, but bias correction methods should be applied to reduce errors for chl-a values.

VIIRS AND MODIS AQUA

VIIRS performed poorly in our study, having a different outcome than other validation studies with this sensor. Studies in the South Java Sea and inland Chinese lakes showed that VIIRS gave commendable *in situ* correlations (i.e., Jiang et al. 2020; $R^2 = 0.76$). However, both studies used VIIRS data that had been processed to finer spatial resolutions (i.e., 375m and 750m), when compared to the one-km resolution in this study (Jiang et al., 2020; Nuris et al., 2015). MODIS Aqua also performed poorly in our study, likely due to the aging of the instruments, far exceeding their expected six-year lifespan (Angal et al., 2023). The accuracy of MODIS Aqua is in line with a recent comparison in similar Case 2 waters that found that the OC3M algorithm with MODIS Aqua data also performed poorly ($R^2 = 0.01$) (Abbas et al., 2019). An earlier study found that, while MODIS Aqua could reasonably estimate chl-a at concentrations from 2 to 50 mg/m³ in Case 2 waters (similar to M1), it tended to lose sensitivity below 20 mg/m³, whereas our data found that accuracy was lost at higher chl-a concentrations

(Gitelson et al., 2009). The performance of VIIRS and MODIS Aqua in this study highlighted the difficulty of using coarse-resolution data and global algorithms derived from Case 1 waters on coastal Case 2 application. These results suggest that users should avoid both sensors (CIA) unless they improve their calibration.

VARIABLE WATERS IN MONTEREY BAY

The coastal waters of Monterey Bay are highly dynamic. The varied performance of sensors and algorithms in this study can be largely attributed to the highly productive coastal nature of Monterey Bay and the seasonal dynamics of upwelling and algal productivity. The increased presence of CDOM, NAPs, and concentrated algal presence can confound algorithms that rely heavily on the blue, green, red and near-infrared wavelengths, which likely explains the varied results that generally correlate with the sophistication of the algorithm used, rather than the spectral capacity of the sensor (Ali et al., 2016; Dall'Olmo and Gitelson, 2005; Gitelson et al., 2009; Herman, 1999). Another reason for the difference in sensors is due to the multiple atmospheric corrections for each sensor. This is a complicated concept as sensors can have various chl-a outputs depending on the atmospheric correction used, such as MODIS Aqua with the use of near infrared, the shortwave infrared and the management unit of the north seas mathematical models corrections (Carswell et al., 2017). Since these vary by sensor in addition to the algorithm, bands and resolutions, it is difficult to have an ideal comparison of satellite chl-a to *in situ* chl-a. Another potential avenue for future research would be to incorporate the Santa Cruz Wharf data, which are collected more frequently than M1 or C1. However, this area also represents more 'extreme' Case 2 waters than C1. The Santa Cruz Wharf may aid the match-up count of all sensors, which was limited in this study, with only a total of six instances across the total focus period in which all four sensors imaged the Monterey Bay area on the same day. Our results support the need for a regional algorithm for the Monterey Bay (ideally for S3), especially considering the extent of scientific research in the area. Additionally, other infrared/red band algorithms (i.e., maximum

chlorophyll index and fluorescence line height) should be tested. The higher resolution of these sensors can support finer submesoscale studies for the region. Furthermore, considering the extensive databases behind these sensors and their performance in this study, all platforms (with the right algorithms) could easily be utilized to quantitatively monitor Monterey Bay (Gitelson et al., 2009).

CONCLUSION

Overall, our study found that OC-CCI and S3, regardless of the applied algorithm, have considerable potential for retrieving chl-a values in Monterey Bay, adding to our understanding of smaller-scale (~300m) processes. This capability can be attributed to their higher spatial resolution, especially when compared to VIIRS and MODIS Aqua, which, despite a coarser spatial resolution, maintain a regular temporal resolution, having a proven reliability that could see a total combined dataset of up to 40 years (Xiong and Butler, 2020). S3 seems to be situated within the ideal trade-off point between reasonably high temporal and spatial resolution, which is why the sensor is one of the most suited to estimate chl-a in Monterey Bay out of the four tested ones. Likewise, OC-CCI, a blended product, can also provide a reasonable temporal and spatial resolution trade-off. However, upcoming products from the NASA plankton, aerosol, cloud, ocean ecosystem and geosynchronous littoral imaging and monitoring radiometer sensors, in addition to other high-resolution sensors such as Landsat 8 or Landsat 9, would likely be comparable or outperform the S3 and OC-CCI products. These newer sensors will be beneficial in their capability of understanding high resolution oceanographic processes, which is also important to improve the estimation of coastal chl-a concentrations and, ultimately, productivity. Future research pertaining to RS in Monterey Bay should firstly investigate the accuracy of S2 by obtaining more *in situ* match ups. This could be achieved by Santa Cruz Wharf data. Other atmospheric corrections and algorithms should also be applied to S2 and S3, alongside other sensors such as Landsat 8 and Landsat 9, to evaluate their respective chl-a

retrieval accuracies. This work is required to improve coastal ocean process studies. Given the focus on oceanography in heavily researched areas such as Monterey Bay, it is crucial to have reliable and accurate fine-scale estimates of chl-a among other products that would help derive submesoscale oceanographic processes.

DATA AVAILABILITY STATEMENT

All data were accessed via open-source repositories online and can also be provided upon request by the corresponding author.

SUPPLEMENTARY MATERIAL

Supplementary material can found at <https://zenodo.org/records/15509963>

ACKNOWLEDGEMENTS

The first author would like to extend the biggest word of thanks to his supervisors Lael Wakamatsu and Andrew Fischer, who dedicated an immense amount of time to help him with this study. Their patience, understanding and support from start to finish and beyond was extremely helpful for him as he has learned many new skills from this project because of them.

We would like to thank Francisco Chavez and the Biological Oceanography Group at MBARI for providing the *in situ* chlorophyll data a M1 and C1.

We would also like to thank John Ryan from MBARI for help in the conceptualization of the project.

Lastly, we would like to thank Alex Fraser for his edits and suggestions on the manuscript.

Reviewer comments significantly improved the manuscript.

FUNDING

No funding was required for this study.

AUTHOR CONTRIBUTIONS

E.S.: Methodology, Software, Validation, Formal Analysis, Investigation, Data Curation, Writing – Original Draft, Visualization, Project Administration.

A.F. & L.W.: Conceptualization, Methodology, Software, Resources, Writing – Review & Editing, Supervision.

CONFLICT OF INTEREST

The authors declare no conflict of interest.

REFERENCES

- Abbas, M. M., Melesse, A. M., Scinto, L. J. & Rehage, J. S. 2019. Satellite Estimation of Chlorophyll-a Using Moderate Resolution Imaging Spectroradiometer (MODIS) Sensor in Shallow Coastal Water Bodies: Validation and Improvement. *Water*, 11(8), 1621. DOI: <https://doi.org/10.3390/W11081621>
- Al-Naimi, N., Raitsos, D. E., Ben-Hamadou, R. & Soliman, Y. 2017. Evaluation of Satellite Retrievals of Chlorophyll-a in the Arabian Gulf. *Remote Sensing*, 9(3), 301. DOI: <https://doi.org/10.3390/RS9030301>
- Ali, K. A., Ortiz, J., Bonini, N., Shuman, M. & Sydow, C. 2016. Application of Aqua MODIS sensor data for estimating chlorophyll a in the turbid Case 2 waters of Lake Erie using bio-optical models. *GI Science and Remote Sensing*, 53(4), 483–505. DOI: <https://doi.org/10.1080/15481603.2016.1177248>
- Angal, A., Xiong, X., Twedt, K., Chang, T., Geng, X., Aldoretta, E. & Díaz, C. P. 2023. Status of the Terra and Aqua Modis Collection 7 L1B. *IGARSS 2023 - 2023 IEEE International Geoscience and Remote Sensing Symposium*, 4466–4469. DOI: <https://doi.org/10.1109/IGARSS52108.2023.10283303>
- Anspers, A. & Alikas, K. 2018. Retrieval of Chlorophyll a from Sentinel-2 MSI Data for the European Union Water Framework Directive Reporting Purposes. *Remote Sensing*, 11(1), 64. DOI: <https://doi.org/10.3390/RS11010064>
- Azmi, S., Agarwadkar, Y., Bhattacharya, M., Apte, M. & Inamdar, A. 2015. Indicator Based Ecological Health Analysis Using Chlorophyll and Sea Surface Temperature Along with Fish Catch Data off Mumbai Coast. *Turkish Journal of Fisheries and Aquatic Sciences*, 15(4), 923–930. DOI: https://doi.org/10.4194/1303-2712-V15_4_16
- Barnes, W. L. & Salomonson, V. V. 1992. MODIS: a global imaging spectroradiometer for the Earth Observing System. *Applications in Optical Science and Engineering*, 10269, 280–302. DOI: <https://doi.org/10.1117/12.161578>
- Basu, S. & Mackey, K. R. M. 2018. Phytoplankton as Key Mediators of the Biological Carbon Pump: Their Responses to a Changing Climate. *Sustainability*, 10(3), 869. DOI: <https://doi.org/10.3390/SU10030869>
- Binh, N. A., Hoa, P. V., Thao, G. T. P., Duan, H. D., & Thu, P. M. (2022). Evaluation of Chlorophyll-a estimation using Sentinel 3 based on various algorithms in southern coastal Vietnam. *International Journal of Applied Earth Observation and Geoinformation*, 112, 102951. <https://doi.org/10.1016/J.JAG.2022.102951>
- Breaker, L. C. 2005. What's happening in Monterey Bay on seasonal to interdecadal time scales. *Continental Shelf Research*, 25(10), 1159–1193. DOI: <https://doi.org/10.1016/J.CSR.2005.01.003>
- Bricaud, A., Morel, A., Babin, M., Allali, K. & Claustre, H. 1998. Variations of light absorption by suspended particles with chlorophyll a concentration in oceanic (Case 1) waters: Analysis and implications for bio-optical models. *Journal of Geophysical Research: Oceans*, 103(C13), 31033–31044. DOI: <https://doi.org/10.1029/98JC02712>
- Brockmann, C., Doerffer, R., Peters, M., Kerstin, S., Embacher, S. & Ruescas, A. 2016. Evolution of the C2RCC Neural Network for Sentinel 2 and 3 for the Retrieval of Ocean Colour Products in Normal and Extreme Optically Complex Waters. *ESASP*, 740, 54. Available from: <https://ui.adsabs.harvard.edu/abs/2016ESASP.740E..54B/abstract>. Access date: May 5 2025.
- Campbell, J. W. 1995. The lognormal distribution as a model for bio-optical variability in the sea. *Journal of Geophysical Research: Oceans*, 100(C7), 13237–13254. DOI: <https://doi.org/10.1029/95JC00458>
- Carswell, T., Costa, M., Young, E., Komick, N., Gower, J. & Sweeting, R. 2017. Evaluation of MODIS-Aqua Atmospheric Correction and Chlorophyll Products of Western North American Coastal Waters Based on 13 Years of Data. *Remote Sensing*, 9(10), 1063. DOI: <https://doi.org/10.3390/RS9101063>
- Cazzaniga, I., Bresciani, M., Colombo, R., Bella, V. Della, Padula, R. & Giardino, C. 2019. A comparison of Sentinel-3-OLCI and Sentinel-2-MSI-derived Chlorophyll-a maps for two large Italian lakes. *Remote Sensing Letters*, 10(10), 978–987. DOI: <https://doi.org/10.1080/2150704X.2019.1634298>
- Chavez, F. P. 1996. *Forcing and biological impact of onset of the 1992 El Nino in central California*, 23, 265–268. DOI: <https://doi.org/10.1029/96GL00017>
- Chen, J., Zhang, M., Cui, T. & Wen, Z. 2013. A review of some important technical problems in respect of satellite remote sensing of chlorophyll - A concentration in coastal waters. *IEEE Journal of Selected Topics in Applied Earth Observations and Remote Sensing*, 6(5), 2275–2289. DOI: <https://doi.org/10.1109/JSTARS.2013.2242845>
- Chen, J., Zhu, W., Tian, Y. Q., Yu, Q., Zheng, Y. & Huang, L. 2017. Remote estimation of colored dissolved organic matter and chlorophyll-a in Lake Huron using Sentinel-2 measurements. *Journal of Applied Remote Sensing*, 11(3), 036007. DOI: <https://doi.org/10.1117/1.JRS.11.036007>
- Dall'Olmo, G. & Gitelson, A. A. 2005. Effect of bio-optical parameter variability on the remote estimation of chlorophyll-a concentration in turbid productive waters: experimental results. *Applied Optics*, 44(3), 412–422. DOI: <https://doi.org/10.1364/AO.44.000412>
- Darecki, M., Weeks, A., Sagan, S., Kowalczyk, P. & Kaczmarek, S. 2003. Optical characteristics of two contrasting Case 2 waters and their influence on remote sensing algorithms. *Continental Shelf Research*, 23(3–4), 237–250. DOI: [https://doi.org/10.1016/S0278-4343\(02\)00222-4](https://doi.org/10.1016/S0278-4343(02)00222-4)
- Divya, M., Dinesh Kumar, S., Krishnaveni, N. & Santhanam, P. 2018. A study of carbon sequestration by phytoplankton. *Basic and Applied Phytoplankton Biology*, 277–284. DOI: https://doi.org/10.1007/978-981-10-7938-2_15
- Friedland, K. D., Stock, C., Drinkwater, K. F., Link, J. S., Leaf, R. T., Shank, B. V., Rose, J. M., Pilskaln, C. H. & Fogarty, M. J. 2012. Pathways between Primary Production and Fisheries Yields of Large Marine Ecosystems. *PLOS ONE*, 7(1), e28945. DOI: <https://doi.org/10.1371/JOURNAL.PONE.0028945>
- Giardino, C., Bresciani, M., Stroppiana, D., Oggioni, A. & Morabito, G. 2014. Optical remote sensing of lakes: an

- overview on Lake Maggiore. *Journal of Limnology*, 73(1), 201–214. DOI: <https://doi.org/10.4081/jlimnol.2014.817>
- Gitelson, A. A., Gurlin, D., Moses, W. J. & Barrow, T. 2009. A bio-optical algorithm for the remote estimation of the chlorophyll-a concentration in Case 2 waters. *Environmental Research Letters*, 4(4), 045003. DOI: <https://doi.org/10.1088/1748-9326/4/4/045003>
- Goffredi, S. K., Paull, C. K., Fulton-Bennett, K., Hurtado, L. A. & Vrijenhoek, R. C. 2004. Unusual benthic fauna associated with a whale fall in Monterey Canyon, California. *Deep Sea Research Part I: Oceanographic Research Papers*, 51(10), 1295–1306. DOI: <https://doi.org/10.1016/J.DSR.2004.05.009>
- Ha, N. T. T., Thao, N. T. P., Koike, K. & Nhuan, M. T. 2017. Selecting the Best Band Ratio to Estimate Chlorophyll-a Concentration in a Tropical Freshwater Lake Using Sentinel 2A Images from a Case Study of Lake Ba Be (Northern Vietnam). *ISPRS International Journal of Geo-Information*, 6(9), 290. DOI: <https://doi.org/10.3390/IJGI6090290>
- Herman, G. 1999. Optical Teledetection of Chlorophyll a in Turbid Inland Waters. *Environmental Science and Technology*, 33(7), 1127–1132. DOI: <https://doi.org/10.1021/es9809657>
- Holm-Hansen, O., Lorenzen, C. J., Holmes, R. W. & Strickland, J. D. H. 1965. Fluorometric Determination of Chlorophyll. *ICES Journal of Marine Science*, 30(1), 3–15. DOI: <https://doi.org/10.1093/ICESJMS/30.1.3>
- Hu, C., Lee, Z. & Franz, B. 2012. Chlorophyll a algorithms for oligotrophic oceans: A novel approach based on three-band reflectance difference. *Journal of Geophysical Research: Oceans*, 117(C1). DOI: <https://doi.org/10.1029/2011JC007395>
- Ivanda, A., Šerić, L., Bugarić, M., & Braović, M. (2021). Mapping Chlorophyll-a Concentrations in the Kaštela Bay and Brač Channel Using Ridge Regression and Sentinel-2 Satellite Images. *Electronics* 2021, 10(23), 3004. <https://doi.org/10.3390/ELECTRONICS10233004>
- Jackson, T. 2020. Product user guide for v5.0 dataset. *D4.2. ESA*. Available from: <https://docs.pml.space/share/s/okB2fOuPT7Cj2r4C5sppDg>. Access date: May 5 2025
- Jiang, G., Loiselle, S. A., Yang, D., Ma, R., Su, W. & Gao, C. 2020. Remote estimation of chlorophyll a concentrations over a wide range of optical conditions based on water classification from VIIRS observations. *Remote Sensing of Environment*, 241, 111735. DOI: <https://doi.org/10.1016/J.RSE.2020.111735>
- Joint, I. & Groom, S. B. 2000. Estimation of phytoplankton production from space: current status and future potential of satellite remote sensing. *Journal of Experimental Marine Biology and Ecology*, 250(1–2), 233–255. DOI: [https://doi.org/10.1016/S0022-0981\(00\)00199-4](https://doi.org/10.1016/S0022-0981(00)00199-4)
- Kahru, M., Kudela, R. M., Anderson, C. R. & Mitchell, B. G. 2015. Optimized Merger of Ocean Chlorophyll Algorithms of MODIS-Aqua and VIIRS. *IEEE Geoscience and Remote Sensing Letters*, 12(11), 2282–2285. DOI: <https://doi.org/10.1109/LGRS.2015.2470250>
- Lin, J., Cao, W., Wang, G., Zhou, W., Sun, Z. & Zhao, W. 2014. Inversion of bio-optical properties in the coastal upwelling waters of the northern South China Sea. *Continental Shelf Research*, 85, 73–84. DOI: <https://doi.org/10.1016/J.CSR.2014.06.001>
- Mansergh, S. & Zehr, J. P. 2014. Vibrio diversity and dynamics in the Monterey Bay upwelling region. *Frontiers in Microbiology*, 5, 48. DOI: <https://doi.org/10.3389/FMICB.2014.00048>
- Manzer, C. R., Connolly, T. P., McPhee-Shaw, E. & Smith, G. J. 2019. Physical factors influencing phytoplankton abundance in southern Monterey Bay. *Continental Shelf Research*, 180, 1–13. DOI: <https://doi.org/10.1016/J.CSR.2019.04.007>
- Markelin, L., Simis, S. G. H., Hunter, P. D., Spyarakos, E., Tyler, A. N., Clewley, D. & Groom, S. 2016. Atmospheric Correction Performance of Hyperspectral Airborne Imagery over a Small Eutrophic Lake under Changing Cloud Cover. *Remote Sensing*, 9(1), 2. DOI: <https://doi.org/10.3390/RS9010002>
- Morel, A., Gentili, B., Claustre, H., Babin, M., Bricaud, A., Ras, J. & Tièche, F. 2007. Optical properties of the “clearest” natural waters. *Limnology and Oceanography*, 52(1), 217–229. DOI: <https://doi.org/10.4319/LO.2007.52.1.0217>
- Morel, A. & Maritorena, S. 2001. Bio-optical properties of oceanic waters: A reappraisal. *Journal of Geophysical Research: Oceans*, 106(C4), 7163–7180. DOI: <https://doi.org/10.1029/2000JC000319>
- Morel, A. & Prieur, L. 1977. Analysis of variations in ocean color1. *Limnology and Oceanography*, 22(4), 709–722. DOI: <https://doi.org/10.4319/LO.1977.22.4.0709>
- Moutzouris-Sidiris, I. & Topouzelis, K. 2021. Assessment of Chlorophyll-a concentration from Sentinel-3 satellite images at the Mediterranean Sea using CMEMS open source in situ data. *Open Geosciences*, 13(1), 85–97. DOI: <https://doi.org/10.1515/GEO-2020-0204>
- Nima, C., Frette, Ø., Hamre, B., Erga, S. R., Chen, Y. C., Zhao, L., Sørensen, K., Norli, M., Stamnes, K. & Stamnes, J. J. 2016. Absorption properties of high-latitude Norwegian coastal water: The impact of CDOM and particulate matter. *Estuarine, Coastal and Shelf Science*, 178, 158–167. DOI: <https://doi.org/10.1016/J.ECSS.2016.05.012>
- Nuris, R., Gaol, J. & Prayogo, T. 2015. Chlorophyll-a Concentrations Estimation from Aqua Modis and VIIRS-NPP Satellite Sensors in South Java Sea Waters - Repositori LAPAN. *International Journal of Remote Sensing and Earth Sciences*, 12(1), 63–70. Available from: <http://repositori.lapan.go.id/1224/>. Access date: May 5 2025.
- O'Reilly, J. E., Maritorena, S., Mitchell, B. G., Siegel, D. A., Carder, K. L., Garver, S. A., Kahru, M. & McClain, C. 1998. Ocean color chlorophyll algorithms for SeaWiFS. *Journal of Geophysical Research: Oceans*, 103(C11), 24937–24953. DOI: <https://doi.org/10.1029/98JC02160>
- Orlandi, M., Silvio Marzano, F., & Cimini, D. (2018). Remote sensing of water quality indexes from Sentinel-2 imagery: development and validation around Italian river estuaries. *20th EGU General Assembly*, 20, 19808. <https://ui.adsabs.harvard.edu/abs/2018EGUGA..2019808O/abstract>
- Parsons, T. R., Maita, Y., & Lalli, C. M. (1984). Determination of Chlorophylls and Total Carotenoids: Spectrophotometric Method. *A Manual of Chemical &*

- Biological Methods for Seawater Analysis*, 101–104. <https://doi.org/10.1016/B978-0-08-030287-4.50032-3>
- Pennington, T. J. & Chavez, F. P. 2000. Seasonal fluctuations of temperature, salinity, nitrate, chlorophyll and primary production at station H3/M1 over 1989–1996 in Monterey Bay, California. *Deep Sea Research Part II: Topical Studies in Oceanography*, 47(5–6), 947–973. DOI: [https://doi.org/10.1016/S0967-0645\(99\)00132-0](https://doi.org/10.1016/S0967-0645(99)00132-0)
- Pirasteh, S., Mollaei, S., Fathollahi, S. N. & Li, J. 2020. Estimation of Phytoplankton Chlorophyll-a Concentrations in the Western Basin of Lake Erie Using Sentinel-2 and Sentinel-3 Data. *Canadian Journal of Remote Sensing*, 46(5), 585–602. DOI: <https://doi.org/10.1080/07038992.2020.1823825>
- Polimene, L., Sailley, S., Clark, D., Mitra, A. & Allen, J. I. 2017. Biological or microbial carbon pump? The role of phytoplankton stoichiometry in ocean carbon sequestration. *Journal of Plankton Research*, 39(2), 180–186. DOI: <https://doi.org/10.1093/PLANKT/FBW091>
- Reji, L., Tolar, B. B., Chavez, F. P. & Francis, C. A. 2020. Depth-Differentiation and Seasonality of Planktonic Microbial Assemblages in the Monterey Bay Upwelling System. *Frontiers in Microbiology*, 11, 1075. DOI: <https://doi.org/10.3389/FMICB.2020.01075>
- Rosenfeld, L. K., Schwing, F. B., Garfield, N. & Tracy, D. E. 1994. Bifurcated flow from an upwelling center: a cold water source for Monterey Bay. *Continental Shelf Research*, 14(9), 931–964. DOI: [https://doi.org/10.1016/0278-4343\(94\)90058-2](https://doi.org/10.1016/0278-4343(94)90058-2)
- Ryan, J. P., Davis, C. O., Tuffillaro, N. B., Kudela, R. M. & Gao, B.-C. 2014. Application of the Hyperspectral Imager for the Coastal Ocean to Phytoplankton Ecology Studies in Monterey Bay, CA, USA. *Remote Sensing*, 6(2), 1007–1025. DOI: <https://doi.org/10.3390/RS6021007>
- Ryan, J. P., Fischer, A. M., Kudela, R. M., Gower, J. F. R., King, S. A., Marin, R. & Chavez, F. P. 2009. Influences of upwelling and downwelling winds on red tide bloom dynamics in Monterey Bay, California. *Continental Shelf Research*, 29(5–6), 785–795. DOI: <https://doi.org/10.1016/J.CSR.2008.11.006>
- Sathyendranath, S., Brewin, B., Mueller, D., Doerffer, R., Krasemann, H., Melin, F., Brockmann, C., Fomferra, N., Peters, M., Grant, M., Steinmetz, F., Deschamps, P.-Y., Swinton, J., Smyth, T., Werdell, J., Franz, B., Maritorea, S., Devred, E., Lee, Z., Hu, C. & Regner, P. 2012. Ocean Colour Climate Change Initiative - Approach and initial results. In: *2012 IEEE International Geoscience and Remote Sensing Symposium*, 1, 2024–2027. Munich, Germany: IEEE. DOI: <https://doi.org/10.1109/IGARSS.2012.6350979>
- Sathyendranath, S.; Jackson, T.; Brockmann, C.; Brotas, V.; Calton, B.; Chuprin, A.; Clements, O.; Cipollini, P.; Danne, O.; Dingle, J.; Donlon, C.; Grant, M.; Groom, S.; Krasemann, H.; Lavender, S.; Mazeran, C.; Mélin, F.; Müller, D.; Steinmetz, F.; Vale, T. 2023. Dataset Record: ESA Ocean Colour Climate Change Initiative (Ocean_Colour_cci): Monthly climatology of global ocean colour data products at 4km resolution, Version 6.0. *NERC EDS Centre for Environmental Analysis*. DOI: <https://doi.org/10.5285/5011d22aae5a4671b0cbc7d05c56c4f0>
- Schiller, H. & Doerffer, R. 1999. Neural network for emulation of an inverse model operational derivation of Case II water properties from MERIS data. *International Journal of Remote Sensing*, 20(9), 1735–1746. DOI: <https://doi.org/10.1080/014311699212443>
- Schueler, C. F., Clement, J. E., Ardanuy, P. E., Welsch, C., DeLuccia, F. & Swenson, H. 2002. NPOESS VIIRS sensor design overview. *International Symposium on Optical Science and Technology*, 4483, 11–23. DOI: <https://doi.org/10.1117/12.453451>
- Shaik, I., Mohammad, S., Nagamani, P. V., Begum, S. K., Kayet, N., & Varaprasad, D. (2021). Assessment of chlorophyll-a retrieval algorithms over Kakinada and Yanam turbid coastal waters along east coast of India using Sentinel-3A OLCI and Sentinel-2A MSI sensors. *Remote Sensing Applications: Society and Environment*, 24, 100644. <https://doi.org/10.1016/J.RSASE.2021.100644>
- Soomets, T., Uudeberg, K., Jakovels, D., Brauns, A., Zagars, M. & Kutser, T. 2020. Validation and Comparison of Water Quality Products in Baltic Lakes Using Sentinel-2 MSI and Sentinel-3 OLCI Data. *Sensors*, 20(3), 742. DOI: <https://doi.org/10.3390/S20030742>
- Sòria-Perpinyà, X., Vicente, E., Urrego, P., Pereira-Sandoval, M., Tenjo, C., Ruíz-Verdú, A., Delegido, J., Soria, J. M., Peña, R. & Moreno, J. 2021. Validation of Water Quality Monitoring Algorithms for Sentinel-2 and Sentinel-3 in Mediterranean Inland Waters with In Situ Reflectance Data. *Water*, 13(5), 686. DOI: <https://doi.org/10.3390/W13050686>
- Sorrell, B. K., Hawes, I., Safi, K., Moses, W. J., Saprygin, V., Gitelson, A. A., Gurlin, D. & Barrow, T. 2009. A bio-optical algorithm for the remote estimation of the chlorophyll-a concentration in Case 2 waters. *Environ. Res. Lett*, 4, 5. DOI: <https://doi.org/10.1088/1748-9326/4/4/045003>
- Staehr, S. U., Holbach, A. M., Markager, S., & Staehr, P. A. U. (2023). Exploratory study of the Sentinel-3 level 2 product for monitoring chlorophyll-a and assessing ecological status in Danish seas. *Science of The Total Environment*, 897, 165310. <https://doi.org/10.1016/J.SCITOTENV.2023.165310>
- Syariz, M. A., Lin, C. H. & Blanco, A. C. 2019. Chlorophyll-a Concentration Retrieval Using Convolutional Neural Networks in Laguna Lake, Philippines. *International Archives of the Photogrammetry, Remote Sensing and Spatial Information Sciences - ISPRS Archives*, 42(4/W19), 401–405. DOI: <https://doi.org/10.5194/ISPRS-ARCHIVES-XLII-4-W19-401-2019>
- Syariz, M. A., Lin, C. H., Van Nguyen, M., Jaelani, L. M. & Blanco, A. C. 2020. WaterNet: A Convolutional Neural Network for Chlorophyll-a Concentration Retrieval. *Remote Sensing*, 12(12), 1966. DOI: <https://doi.org/10.3390/RS12121966>
- Theenathayalan, V., Sathyendranath, S., Kulk, G., Menon, N., George, G., Abdulaziz, A., Selmes, N., Brewin, R. J. W., Rajendran, A., Xavier, S. & Platt, T. 2022. Regional Satellite Algorithms to Estimate Chlorophyll-a and Total Suspended Matter Concentrations in Vembanad Lake. *Remote Sensing*, 14(24), 6404. DOI: <https://doi.org/10.3390/RS14246404>
- Thomson, R. E. & Krassovski, M. V. 2010. Poleward reach of the California Undercurrent extension. *Journal*

- of *Geophysical Research: Oceans*, 115(C9), 9027. DOI: <https://doi.org/10.1029/2010JC006280>
- Tilstone, G. H., Pardo, S., Dall'Olmo, G., Brewin, R. J. W., Nencioli, F., Dessailly, D., Kwiatkowska, E., Casal, T. & Donlon, C. 2021. Performance of Ocean Colour Chlorophyll a algorithms for Sentinel-3 OLCI, MODIS-Aqua and Suomi-VIIRS in open-ocean waters of the Atlantic. *Remote Sensing of Environment*, 260, 112444. DOI: <https://doi.org/10.1016/J.RSE.2021.112444>
- Torbick, N., Hu, F., Zhang, J., Qi, J., Zhang, H. & Becker, B. 2008. Mapping Chlorophyll-a Concentrations in West Lake, China using Landsat 7 ETM+. *Journal of Great Lakes Research*, 34(3), 559–565. DOI: [https://doi.org/10.3394/0380-1330\(2008\)34\[559:mcciw\]2.0.co;2](https://doi.org/10.3394/0380-1330(2008)34[559:mcciw]2.0.co;2)
- Valente, A., Sathyendranath, S., Brotas, V., Groom, S., Grant, M., Jackson, T., Chuprin, A., Taberner, M., Airs, R., Antoine, D., Arnone, R., Balch, W. M., Barker, K., Barlow, R., Bélanger, S., Berthon, J. F., Beşiktepe, Ş., Borsheim, Y., Bracher, A., Brando, V., Brewin, R. J. W., Canuti, E., Chavez, F. P., Cianca, A., Claustre, H., Clementson, L., Crout, R., Ferreira, A., Freeman, S., Frouin, R., García-Soto, C., Gibb, S. W., Goericke, R., Gould, R., Guillocheau, N., Hooker, S. B., Hu, C., Kahru, M., Kampel, M., Klein, H., Kratzer, S., Kudela, R., Ledesma, J., Lohrenz, S., Loisel, H., Mannino, A., Martinez-Vicente, V., Matrai, P., Mckee, D., Mitchell, B. G., Moisan, T., Montes, E., Muller-Karger, F., Neeley, A., Novak, M., O'dowd, L., Ondrusek, M., Platt, T., Poulton, A. J., Repecaud, M., Röttgers, R., Schroeder, T., Smyth, T., Smythe-Wright, D., Sosik, H. M., Thomas, C., Thomas, R., Tilstone, G., Tracana, A., Twardowski, M., Vellucci, V., Voss, K., Werdell, J., Wernand, M., Wojtasiewicz, B., Wright, S. & Zibordi, G. 2022. A compilation of global bio-optical in situ data for ocean colour satellite applications – version three. *Earth System Science Data*, 14(12), 5737–5770. DOI: <https://doi.org/10.5194/ESSD-14-5737-2022>
- Vanhellemont, Q. & Ruddick, K. 2021. Atmospheric correction of Sentinel-3/OLCI data for mapping of suspended particulate matter and chlorophyll-a concentration in Belgian turbid coastal waters. *Remote Sensing of Environment*, 256, 112284. DOI: <https://doi.org/10.1016/J.RSE.2021.112284>
- Wakamatsu, L., Britten, G. L., Styles, E. J. & Fischer, A. M. 2022. Chlorophyll-a and Sea Surface Temperature Changes in Relation to Paralytic Shellfish Toxin Production off the East Coast of Tasmania, Australia. *Remote Sensing*, 14(3), 665. DOI: <https://doi.org/10.3390/RS14030665>
- Werdell, P. J., Franz, B. A. & Bailey, S. W. 2010. Evaluation of shortwave infrared atmospheric correction for ocean color remote sensing of Chesapeake Bay. *Remote Sensing of Environment*, 114(10), 2238–2247. DOI: <https://doi.org/10.1016/J.RSE.2010.04.027>
- Xiong, X. & Butler, J. J. 2020. MODIS and VIIRS Calibration History and Future Outlook. *Remote Sensing*, 12(16), 2523. DOI: <https://doi.org/10.3390/RS12162523>